

52. IWK

Internationales Wissenschaftliches Kolloquium
International Scientific Colloquium



PROCEEDINGS

| 10 - 13 September 2007

FACULTY OF COMPUTER SCIENCE AND AUTOMATION



COMPUTER SCIENCE MEETS AUTOMATION

VOLUME II

Session 6 - Environmental Systems: Management and Optimisation

**Session 7 - New Methods and Technologies for Medicine and
Biology**

Session 8 - Embedded System Design and Application

Session 9 - Image Processing, Image Analysis and Computer Vision

Session 10 - Mobile Communications


Session 11 - Education in Computer Science and Automation

Bibliografische Information der Deutschen Bibliothek

Die Deutsche Bibliothek verzeichnet diese Publikation in der deutschen Nationalbibliografie; detaillierte bibliografische Daten sind im Internet über <http://dnb.ddb.de> abrufbar.

ISBN 978-3-939473-17-6

Impressum

- Herausgeber: Der Rektor der Technischen Universität Ilmenau
Univ.-Prof. Dr. rer. nat. habil. Peter Scharff
- Redaktion: Referat Marketing und Studentische Angelegenheiten
Kongressorganisation
Andrea Schneider
Tel.: +49 3677 69-2520
Fax: +49 3677 69-1743
e-mail: kongressorganisation@tu-ilmenau.de
- Redaktionsschluss: Juli 2007
- Verlag: 
Technische Universität Ilmenau/Universitätsbibliothek
Universitätsverlag Ilmenau
Postfach 10 05 65
98684 Ilmenau
www.tu-ilmenau.de/universitaetsverlag
- Herstellung und Auslieferung: Verlagshaus Monsenstein und Vannerdat OHG
Am Hawerkamp 31
48155 Münster
www.mv-verlag.de
- Layout Cover: www.cey-x.de
- Bezugsmöglichkeiten: Universitätsbibliothek der TU Ilmenau
Tel.: +49 3677 69-4615
Fax: +49 3677 69-4602

© Technische Universität Ilmenau (Thür.) 2007

Diese Publikationen und alle in ihr enthaltenen Beiträge und Abbildungen sind urheberrechtlich geschützt. Mit Ausnahme der gesetzlich zugelassenen Fälle ist eine Verwertung ohne Einwilligung der Redaktion strafbar.

Preface

Dear Participants,

Confronted with the ever-increasing complexity of technical processes and the growing demands on their efficiency, security and flexibility, the scientific world needs to establish new methods of engineering design and new methods of systems operation. The factors likely to affect the design of the smart systems of the future will doubtless include the following:

- As computational costs decrease, it will be possible to apply more complex algorithms, even in real time. These algorithms will take into account system nonlinearities or provide online optimisation of the system's performance.
- New fields of application will be addressed. Interest is now being expressed, beyond that in "classical" technical systems and processes, in environmental systems or medical and bioengineering applications.
- The boundaries between software and hardware design are being eroded. New design methods will include co-design of software and hardware and even of sensor and actuator components.
- Automation will not only replace human operators but will assist, support and supervise humans so that their work is safe and even more effective.
- Networked systems or swarms will be crucial, requiring improvement of the communication within them and study of how their behaviour can be made globally consistent.
- The issues of security and safety, not only during the operation of systems but also in the course of their design, will continue to increase in importance.

The title "Computer Science meets Automation", borne by the 52nd International Scientific Colloquium (IWK) at the Technische Universität Ilmenau, Germany, expresses the desire of scientists and engineers to rise to these challenges, cooperating closely on innovative methods in the two disciplines of computer science and automation.

The IWK has a long tradition going back as far as 1953. In the years before 1989, a major function of the colloquium was to bring together scientists from both sides of the Iron Curtain. Naturally, bonds were also deepened between the countries from the East. Today, the objective of the colloquium is still to bring researchers together. They come from the eastern and western member states of the European Union, and, indeed, from all over the world. All who wish to share their ideas on the points where "Computer Science meets Automation" are addressed by this colloquium at the Technische Universität Ilmenau.

All the University's Faculties have joined forces to ensure that nothing is left out. Control engineering, information science, cybernetics, communication technology and systems engineering – for all of these and their applications (ranging from biological systems to heavy engineering), the issues are being covered.

Together with all the organizers I should like to thank you for your contributions to the conference, ensuring, as they do, a most interesting colloquium programme of an interdisciplinary nature.

I am looking forward to an inspiring colloquium. It promises to be a fine platform for you to present your research, to address new concepts and to meet colleagues in Ilmenau.



Professor Peter Scharff
Rector, TU Ilmenau



Professor Christoph Ament
Head of Organisation

CONTENTS

	Page
6 Environmental Systems: Management and Optimisation	
T. Bernard, H. Linke, O. Krol A Concept for the long term Optimization of regional Water Supply Systems as a Module of a Decision Support System	3
S. Röhl, S. Hopfgarten, P. Li A groundwater model for the area Darkhan in Kharaa river Th. Bernard, H. Linke, O. Krol basin	11
A. Khatanbaatar Altantuul The need designing integrated urban water management in cities of Mongolia	17
T. Rauschenbach, T. Pfützenreuter, Z. Tong Model based water allocation decision support system for Beijing	23
T. Pfützenreuter, T. Rauschenbach Surface Water Modelling with the Simulation Library ILM-River	29
D. Karimanzira, M. Jacobi Modelling yearly residential water demand using neural networks	35
Th. Westerhoff, B. Scharaw Model based management of the drinking water supply system of city Darkhan in Mongolia	41
N. Buyankhishig, N. Batsukh Pumping well optimi ation in the Shivee-Ovoo coal mine Mongolia	47
S. Holzmüller-Laue, B. Göde, K. Rimane, N. Stoll Data Management for Automated Life Science Applications	51
N. B. Chang, A. Gonzalez A Decision Support System for Sensor Deployment in Water Distribution Systems for Improving the Infrastructure Safety	57
P. Hamolka, I. Vrublevsky, V. Parkoun, V. Sokol New Film Temperature And Moisture Microsensors for Environmental Control Systems	63
N. Buyankhishig, M. Masumoto, M. Aley Parameter estimation of an unconfined aquifer of the Tuul River basin Mongolia	67

M. Jacobi, D. Karimanzira	73
Demand Forecasting of Water Usage based on Kalman Filtering	

7 New Methods and Technologies for Medicine and Biology

J. Meier, R. Bock, L. G. Nyúl, G. Michelson	81
Eye Fundus Image Processing System for Automated Glaucoma Classification	
L. Hellrung, M. Trost	85
Automatic focus depending on an image processing algorithm for a non mydriatic fundus camera	
M. Hamsch, C. H. Igney, M. Vauhkonen	91
A Magnetic Induction Tomography System for Stroke Classification and Diagnosis	
T. Neumuth, A. Pretschner, O. Burgert	97
Surgical Workflow Monitoring with Generic Data Interfaces	
M. Pfaff, D. Woetzel, D. Driesch, S. Toepfer, R. Huber, D. Pohlers, D. Koczan, H.-J. Thiesen, R. Guthke, R. W. Kinne	103
Gene Expression Based Classification of Rheumatoid Arthritis and Osteoarthritis Patients using Fuzzy Cluster and Rule Based Method	
S. Toepfer, S. Zellmer, D. Driesch, D. Woetzel, R. Guthke, R. Gebhardt, M. Pfaff	107
A 2-Compartment Model of Glutamine and Ammonia Metabolism in Liver Tissue	
J. C. Ferreira, A. A. Fernandes, A. D. Santos	113
Modelling and Rapid Prototyping an Innovative Ankle-Foot Orthosis to Correct Children Gait Pathology	
H. T. Shandiz, E. Zahedi	119
Noninvasive Method in Diabetic Detection by Analyzing PPG Signals	
S. V. Drobot, I. S. Asayenok, E. N. Zacepin, T. F. Sergiyenko, A. I. Svirnovskiy	123
Effects of Mm-Wave Electromagnetic Radiation on Sensitivity of Human Lymphocytes to Ionizing Radiation and Chemical Agents in Vitro	

8 Embedded System Design and Application

B. Däne	131
Modeling and Realization of DMA Based Serial Communication for a Multi Processor System	

M. Müller, A. Pacholik, W. Fengler Tool Support for Formal System Verification	137
A. Pretschner, J. Alder, Ch. Meissner A Contribution to the Design of Embedded Control Systems	143
R. Ubar, G. Jervan, J. Raik, M. Jenihhin, P. Ellervee Dependability Evaluation in Fault Tolerant Systems with High-Level Decision Diagrams	147
A. Jutmann On LFSR Polynomial Calculation for Test Time Reduction	153
M. Rosenberger, M. J. Schaub, S. C. N. Töpfer, G. Linß Investigation of Efficient Strain Measurement at Smallest Areas Applying the Time to Digital (TDC) Principle	159
 9 Image Processing, Image Analysis and Computer Vision	
J. Meyer, R. Espiritu, J. Earthman Virtual Bone Density Measurement for Dental Implants	167
F. Erfurth, W.-D. Schmidt, B. Nyuyki, A. Scheibe, P. Saluz, D. Faßler Spectral Imaging Technology for Microarray Scanners	173
T. Langner, D. Kollhoff Farbbasierte Druckbildinspektion an Rundkörpern	179
C. Lucht, F. Gaßmann, R. Jahn Inline-Fehlerdetektion auf freigeformten, texturierten Oberflächen im Produktionsprozess	185
H.-W. Lahmann, M. Stöckmann Optical Inspection of Cutting Tools by means of 2D- and 3D-Imaging Processing	191
A. Melitzki, G. Stanke, F. Weckend Bestimmung von Raumpositionen durch Kombination von 2D-Bildverarbeitung und Mehrfachlinienlasertriangulation - am Beispiel von PKW-Stabilisatoren	197
F. Boochs, Ch. Raab, R. Schütze, J. Traiser, H. Wirth 3D contour detection by means of a multi camera system	203

M. Brandner Vision-Based Surface Inspection of Aeronautic Parts using Active Stereo	209
H. Lettenbauer, D. Weiss X-ray image acquisition, processing and evaluation for CT-based dimensional metrology	215
K. Sickel, V. Daum, J. Hornegger Shortest Path Search with Constraints on Surface Models of In-the-ear Hearing Aids	221
S. Husung, G. Höhne, C. Weber Efficient Use of Stereoscopic Projection for the Interactive Visualisation of Technical Products and Processes	227
N. Schuster Measurement with subpixel-accuracy: Requirements and reality	233
P. Brückner, S. C. N. Töpfer, M. Correns, J. Schnee Position- and colour-accurate probing of edges in colour images with subpixel resolution	239
E. Sparrer, T. Machleidt, R. Nestler, K.-H. Franke, M. Niebelschütz Deconvolution of atomic force microscopy data in a special measurement mode – methods and practice	245
T. Machleidt, D. Kapusi, T. Langner, K.-H. Franke Application of nonlinear equalization for characterizing AFM tip shape	251
D. Kapusi, T. Machleidt, R. Jahn, K.-H. Franke Measuring large areas by white light interferometry at the nanopositioning and nanomeasuring machine (NPM)M)	257
R. Burdick, T. Lorenz, K. Bobey Characteristics of High Power LEDs and one example application in with-light-interferometry	263
T. Koch, K.-H. Franke Aspekte der strukturbasierten Fusion multimodaler Satellitendaten und der Segmentierung fusionierter Bilder	269
T. Riedel, C. Thiel, C. Schmallius A reliable and transferable classification approach towards operational land cover mapping combining optical and SAR data	275
B. Waske, V. Heinzl, M. Braun, G. Menz Classification of SAR and Multispectral Imagery using Support Vector Machines	281

V. Heinzl, J. Franke, G. Menz Assessment of differences in multisensoral remote sensing imageries caused by discrepancies in the relative spectral response functions	287
I. Aksit, K. Bunger, A. Fassbender, D. Frekers, Chr. Gotze, J. Kemenas An ultra-fast on-line microscopic optical quality assurance concept for small structures in an environment of man production	293
D. Hofmann, G. Linss Application of Innovative Image Sensors for Quality Control	297
A. Jablonski, K. Kohrt, M. Bohm Automatic quality grading of raw leather hides	303
M. Rosenberger, M. Schellhorn, P. Bruckner, G. Lin Uncompressed digital image data transfer for measurement techniques using a two wire signal line	309
R. Blaschek, B. Meffert Feature point matching for stereo image processing using nonlinear filters	315
A. Mitsiukhin, V. Pachynin, E. Petrovskaya Hartley Discrete Transform Image Coding	321
S. Hellbach, B. Lau, J. P. Eggert, E. Korner, H.-M. Gro Multi-Cue Motion Segmentation	327
R. R. Alavi, K. Brie Image Processing Algorithms for Using a Moon Camera as Secondary Sensor for a Satellite Attitude Control System	333
S. Bauer, T. Doring, F. Meysel, R. Reulke Traffic Surveillance using Video Image Detection Systems	341
M. A-Megeed Salem, B. Meffert Wavelet-based Image Segmentation for Traffic Monitoring Systems	347
E. Einhorn, C. Schroter, H.-J. Bohme, H.-M. Gro A Hybrid Kalman Filter Based Algorithm for Real-time Visual Obstacle Detection	353
U. Knauer, R. Stein, B. Meffert Detection of opened honeybee brood cells at an early stage	359

10 Mobile Communications

K. Ghanem, N. Zamin-Khan, M. A. A. Kalil, A. Mitschele-Thiel Dynamic Reconfiguration for Distributing the Traffic Load in the Mobile Networks	367
N. Z.-Khan, M. A. A. Kalil, K. Ghanem, A. Mitschele-Thiel Generic Autonomic Architecture for Self-Management in Future Heterogeneous Networks	373
N. Z.-Khan, K. Ghanem, St. Leistritz, F. Liers, M. A. A. Kalil, H. Kärst, R. Böringer Network Management of Future Access Networks	379
St. Schmidt, H. Kärst, A. Mitschele-Thiel Towards cost-effective Area-wide Wi-Fi Provisioning	385
A. Yousef, M. A. A. Kalil A New Algorithm for an Efficient Stateful Address Autoconfiguration Protocol in Ad hoc Networks	391
M. A. A. Kalil, N. Zamin-Khan, H. Al-Mahdi, A. Mitschele-Thiel Evaluation and Improvement of Queueing Management Schemes in Multihop Ad hoc Networks	397
M. Ritzmann Scientific visualisation on mobile devices with limited resources	403
R. Brecht, A. Kraus, H. Krömker Entwicklung von Produktionsrichtlinien von Sport-Live-Berichterstattung für Mobile TV Übertragungen	409
N. A. Tam RCS-M: A Rate Control Scheme to Transport Multimedia Traffic over Satellite Links	421
Ch. Kellner, A. Mitschele-Thiel, A. Diab Performance Evaluation of MIFA, HMIP and HAWAII	427
A. Diab, A. Mitschele-Thiel MIFAv6: A Fast and Smooth Mobility Protocol for IPv6	433
A. Diab, A. Mitschele-Thiel CAMP: A New Tool to Analyse Mobility Management Protocols	439

11 Education in Computer Science and Automation

S. Bräunig, H.-U. Seidel Learning Signal and Pattern Recognition with Virtual Instruments	447
St. Lambeck Use of Rapid-Control-Prototyping Methods for the control of a nonlinear MIMO-System	453
R. Pittschellis Automatisierungstechnische Ausbildung an Gymnasien	459
A. Diab, H.-D. Wuttke, K. Henke, A. Mitschele-Thiel, M. Ruhwedel MAeLE: A Metadata-Driven Adaptive e-Learning Environment	465
V. Zöppig, O. Radler, M. Beier, T. Ströhla Modular smart systems for motion control teaching	471
N. Pranke, K. Froitzheim The Media Internet Streaming Toolbox	477
A. Fleischer, R. Andreev, Y. Pavlov, V. Terzieva An Approach to Personalized Learning: A Technique of Estimation of Learners Preferences	485
N. Tsyrelchuk, E. Ruchaevskaia Innovational pedagogical technologies and the Information educational medium in the training of the specialists	491
Ch. Noack, S. Schwintek, Ch. Ament Design of a modular mechanical demonstration system for control engineering lectures	497

N. Schuster

Measurement with subpixel-accuracy: Requirements and reality

9.4 Image Based 2D- and 3D-Measurement

The accuracy of an image based machine vision installation determines the choice of camera, measuring lens and illumination. Very often, the accuracy is expressed in parts of pixels because the imaging device forms the reference of the measuring arrangement. The unit “pixel” (here PX) guaranties a quick connection to other parameters of the camera like frame rate, required space and process control.

The digital image is the result of a sophisticated process chain which contains 1. the illuminated piece under test, 2. the image formation by the lens, 3. the transfer of light energy in electrical signals by the imaging device, 4. the charge transfer to analog-digital transducer, 5. the analysis of the grey-value image, 6. the subpixel edge detection algorithm. Serious publications name a maximum of accuracy of 1/5 PX ... 1/10 PX [1]. Much smaller values in advertising publications like 1/20 PX ... 1/40 PX ignore the influence of the steps 1-4.

In the following we present investigations in lab environment about the subpixel-accuracy what is referred to a mechanical material measure. This accuracy δN is composed of two parts: the edge detection error ΔN and the calibration error Δc .

1. Method to measure the edge detection error

The distance of two gauge blocks serves as mechanical material measure. The medium distance between gauge blocks is 30 mm, it can be varied in steps of 1/15 PX. Fig. 1 shows this installation.

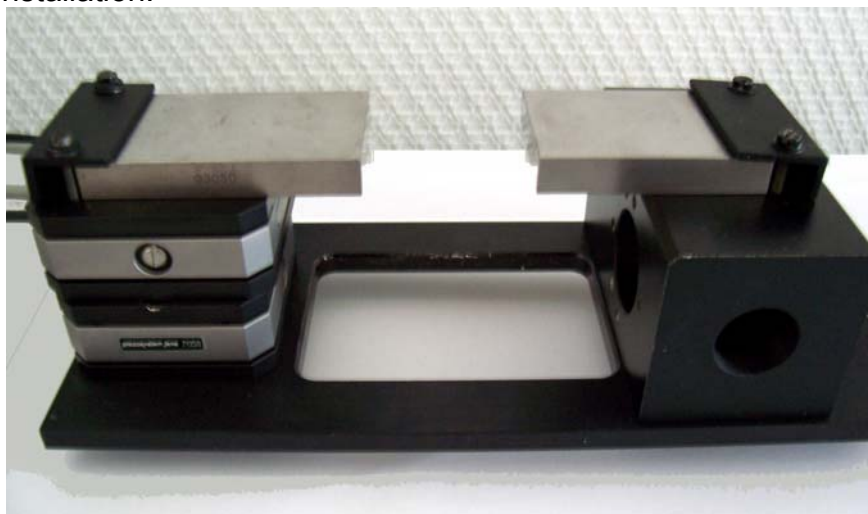


Fig. 1: Material measure to measure the subpixel-accuracy

The gauge-bloc on the right hand side is fixed, the second gauge bloc is mounted on a piezo-moved table. The two gauge blocs have a thickness of 9 mm. They can be driven

in steps of 1 μm with a repeat accuracy of 75 nm.

The window on the bottom side of the stage permits to install different lighting units working in transmitting light. These units illuminate the piece under test in different manner: diffuse or telecentric, monochrome or white.

A telecentric lens T240/0,13 having a maximum field of view of 68 x 51 mm² views from the top side on the two gauge blocks. An entocentric lens would deliver false results in this constellation due to the perspective error.

The principle of measurement of the edge detection error is to compare the translational displacement of gauge blocs with the results of the subpixel edge detection algorithm in the digital image. The gauge bloc distance will be varied in 1/15 parts of one pixel.

Fig. 2 shows typical results: We don't obtain an ideal straight line but rather a lot of line pieces with varying slope. Here, each point represents the average of 7 measurement runs in the corresponding gauge bloc position. The subpixel accuracy follows by interpretation of these curves.

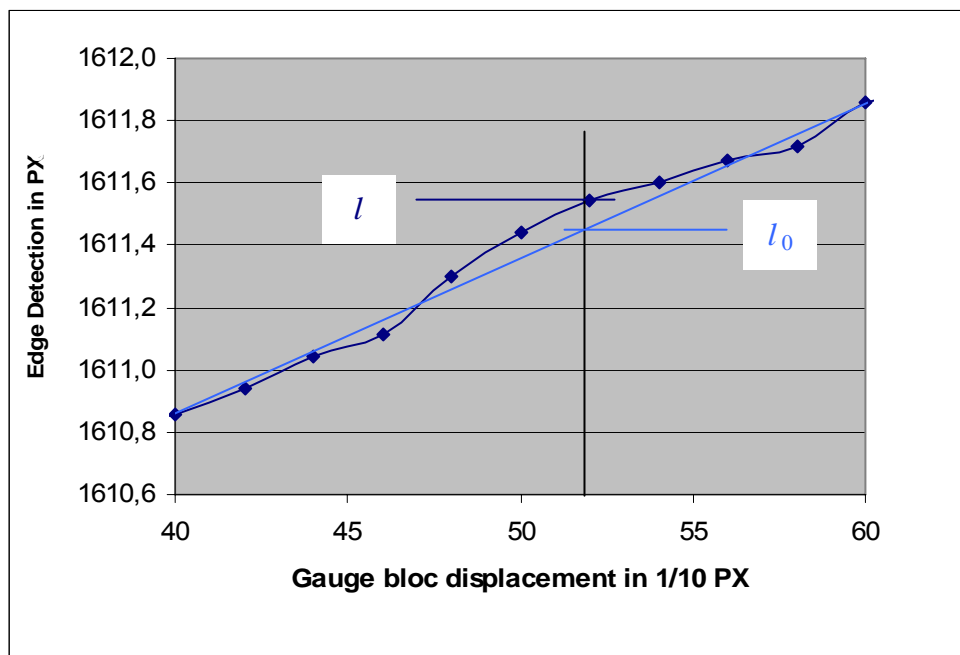


Fig. 2: Edge detection and their linear regression

The edge detection error is the averaged deviation ΔN what is defined by the modulus of differences between the ideal linear regression and the measured value (see Fig. 2):

$$\Delta N = \frac{1}{m} \sum_{i=1}^m l - l_0 \quad (1)$$

while m is the number of gauge bloc positions, l is the result of the subpixel edge detection and l_0 is the ideal length onto the linear regressed straight line.

In the following, we try to find recommendations to save a maximum in subpixel accuracy. For this, we analyze the results of edge detection under different circumstances as direction of edge detection, pixel-pitch and kind of illumination.

2. Aperture of telecentric lens

Fig. 3 shows the aggravating influence of the lens aperture. The gauge bloc is projected by the telecentric lens T240/0,13 on the 2/3"-CCD-matrix of the camera Oscar F810-C at maximum, middle and minimum aperture. Resulting curves disagree.

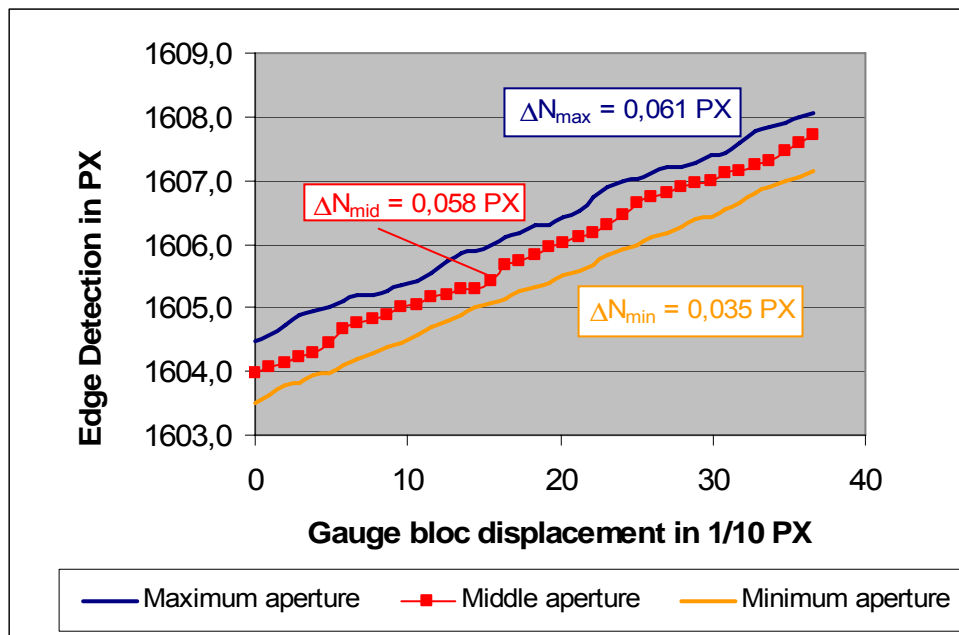


Fig. 3: Edge detection subpixel results versus gauge bloc displacement

Fig. 3 exemplifies the influence of the lens aperture: one pixel difference between the maximum and minimum. The conclusion for the 2D-measurement praxis is evident: Don't change the aperture after calibration.

The smallest deviation from the ideal straight shows the curve at the minimum aperture where the diffraction diffuses the light distribution on the imaging device. This slowly diffused image generates a good condition for the subpixel edge detection. The sharpest and brightest image at the maximum aperture offers the maximum of straight deviation. The average slope of three curves is identical.

3. Illumination color and direction of edge detection

This often discussed problem depends mainly on the geometry of the matrix and of the number of activated light receiving cells. For measuring purposes it is exigent recommended to use an imaging device featuring an equal pixel pitch p' in x' - and y' -direction while x' and y' indicate the axis's of the light sensitive area (see Fig.4).

In the following investigation, we combine the color camera Oscar F810-C having a pixel pitch of $2,8 \mu\text{m}$ in both directions with a telecentric lighting unit TZB60 in different colors. The matrix of the camera F810-C is covered with the Bayer pattern where the half of the cell number is sensible to green, the fourth to red and the other fourth to blue.

White, green, red and blue telecentric lighting units TZB60 are installed on the bottom side of Fig. 1. The quantitative analyze of the edge detection error at different colors corresponds to the number of activated pixel cells: $\Delta N_{\text{white}} = 0,052$, $\Delta N_{\text{green}} = 0,04$, $\Delta N_{\text{red}} = 0,03$, $\Delta N_{\text{blue}} = 0,01$. The white light assures the smallest edge detection error, the blue light the biggest. Due to the color interpolation into the camera, differences of accuracy between colors are diminished. The conclusion for the 2D-measurement praxis is evident: A color camera have to be combined with a white illumination unit.

The often discussed choice of the direction in the edge detection process will be investigated using the white telecentric lighting unit TZB60-W. The digital image is captured by the camera Oscar F810-C. The analyze of 7 test runs in the two axis directions and at 45°.

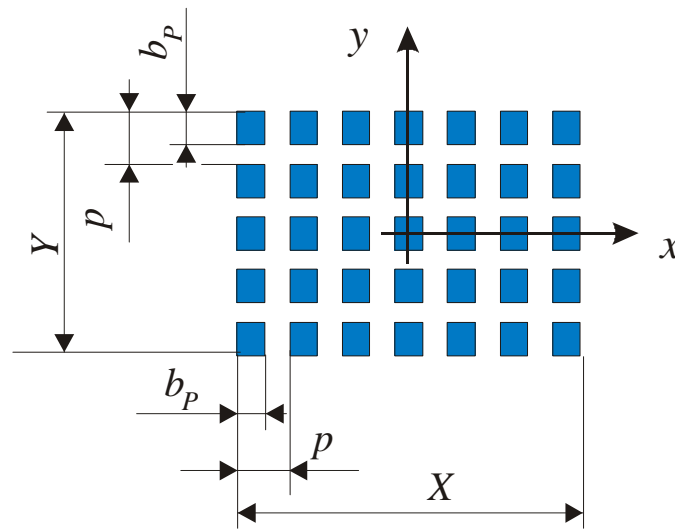


Fig. 4: Preferable matrix geometry for measuring purposes

The edge detection error in different directions is found to $\Delta N_x = 0.040$, $\Delta N_y = 0.04$, $\Delta N_{45^\circ} = 0.051$. The best accuracy follows in x-direction. In y-direction, the edge detection error is 15% higher. Perhaps, it's due to the higher noise level in the column reading than the line reading of the camera CCD. A significant difference is found at the 45° edge detection. Here, the edge detection error is by the factor $\sqrt[4]{2}$ higher than the average of both axial errors. This relation corresponds to the superposition of two no correlated processes. They are the edge detection in both axes.

The recommendation for the 2D-measurement praxis with CCD-imaging devices is to orient the critical dimension to measure in x'-direction (if it possible).

4. Appropriate resolution of the telecentric lens

Very often, the image quality of a telecentric lens has to be “very good”. In the case of the distortion, the specification can be transformed in mm, what gives a clear reference to the required accuracy of the 2D-measuring system.

The specification of appropriate resolution is more complex. It depends on many factors like color of illumination, pixel pitch, interpolation procedures into the camera and edge detection algorithm.

Fig. 5 shows unwelcome results of edge detection what often remain unperceived in practical applications. Only the comparison with an adapted mechanical material measure discloses this kind of irregularity, while the used material measure must correspond to the piece under test in form, surface roughness and color.

These unwelcome results of edge detection in Fig. 5 come from the too high resolution of the telecentric lens. The lens T240/0,13 produces in combination with the Oscar F810-C camera (pixel pitch 2,8 μm) and white telecentric lighting unit likely linear edge detection results having an error $\Delta N \leq 0.01$ (see Fig. 3). Now, we present the combination of the same lens with the monochrome 2/3"-CCD-camera Pictor® M1018 (pixel pitch 6,7 μm) and the telecentric lighting unit TZB60-B. The blue light generated by a LED has a bandwidth of 25 nm. By this means, all residual chromatical aberrations are eliminated.

Beyond of this, the Pictor® M1018 works without an interpolation algorithm between neighbor pixels.

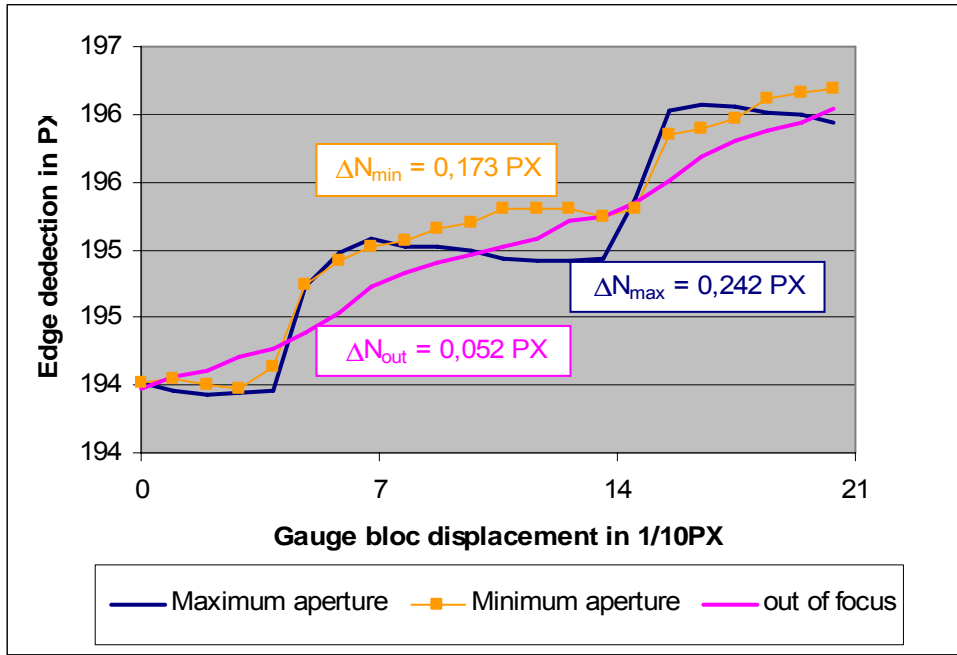


Fig. 5: Edge detection at “to sharp image”

The edge detection error at maximum aperture is four times higher than in the Oscar combination. Respecting the 2,4 times larger pixel pitch in the M1018, the error of accuracy in mm is 10 times larger! At the minimum aperture, this relation increases to twelve. The third curve in Fig.5 confirms the thesis about the “to sharp image”: an object side defocus of 30 mm delivers a likely linear behavior at maximum aperture. The edge detection error of this third curve corresponds to results of all investigated Oscar combinations: $\Delta N_{out} = 0.052$. The investigation of the combination M1018 with the TZB60-W at sharp object position delivers nearly the same edge detection error: $\Delta N_{white} = 0.04$.

For practical applications, the effect of the “to sharp image” is especially malicious because their disclosure demands expensive test arrangements. Beside of this, a traditional engineer of metrology has to accept the effect of a “to sharp image”. A white illuminating unit helps to avoid the “to sharp image” effect.

5. Conclusion

The edge detection error is only one of causes in the 2D-metrology what diminish the accuracy. Their amount depends on the balance of optical resolution, pixel pitch and interpolation runs in the camera. Our investigation under lab conditions delivers a typical value of $\Delta N \approx 1.20$. Adverse effects like the “to sharp image” deteriorate this coefficient up to $\frac{1}{4}$ PX.

The accuracy of the complete 2D-measurement installation δN has to respect the supplement effect of the calibration error Δc . One proposal to calculate the accuracy is

$$\delta N = \Delta N + N \cdot \Delta c = \Delta N + N \cdot \frac{\Delta \beta}{\beta} \quad (2)$$

While N is the size of the piece under test in PX. The last term in Eq.(2) describes the variation of the lateral magnification β during the measuring process while $\Delta \beta$ presents the standard deviation over there. Δc represents e.g. the perspective error of entocentric lenses and the “residual distortion”. They are no correlated errors.

The “residual distortion” implicates that the lens distortion can be electronically compensated. The compensation by symmetrical polynomial approximation in the field yields a residual distortion error between 1/10...1/20 PX [2]. The bilinear approximation in parts of the field of view respects the asymmetrical distortion due to the assembling of lens and camera. Here, the share in Δc depends strongly on the concrete measurement installation.

A method to measure the calibration error Δc is to change the position of the calibration piece in the field of view. Each of typical positions delivers one value of the lateral magnification, and Δc is calculated by (2).

The investigation of the combination T240-lens with Oscar camera in white light permits to quantifier the effect of telecentric illumination versus the classical diffuse back light. The measured calibration error at telecentric illumination is $1000\Delta c_{TZB} = 0.152$, the diffuse back light installation delivers $1000\Delta c_{DBL} = 0.20$ what is poorer. On the other side, the difference of both installations in the edge detection error is smaller: $\Delta N_{TZB} = 0.052$ and $\Delta N_{DBL} = 0.05$. The resultant accuracy is dominated by the calibration error of the diffuse back light: $\delta N_{TZB} = 0.25$ and $\delta N_{DBL} = 0.32$. Practically, a subpixel result of 1/10 PX with the diffuse back light make a false show of accuracy.

The attainable accuracy in the contact less 2D-metrology depends on the actual measurement installation. Expensive test installations based on a mechanical material measure disclose the relations in accuracy. Moreover, the test installation has to present the equivalent condition as the piece under test.

The presented approach distinguishes the edge detection error and the calibration error. Test runs are proposed. The quantitative evaluation suggests that a stable accuracy value of 1/10 PX demand expensive conditions. Values of 1/20 PX or more fine ignore the imponderability between the illuminated piece under test and the digital image to evaluate.

References:

[1] C. Demand, B. Streicher-Abel, P. Waskewitz, *Industrielle Bildverarbeitung*, Springer, Heidelberg 1998, ISBN 3-540-63877-6

[2] N. Schuster, A. Schmidt, “Legende und Wirklichkeit: Messgenauigkeit mittels Subpixel-Interpolation”, in: *Automatisierungsatlas 2006/07*, S. 536-542, TeDo-Verlag Marburg.

Author:

Norbert Schuster
Vision&Control GmbH
Pfüttschbergstr. 14
D-98527 Suhl
Phone: 49/3681/797425
Fax: 49/3681/797465
E-mail: dr.schuster@vision-control.com